



Article citation info:

Hryciów Z, Krasoń W, Wysocki J. Evaluation of the influence of friction in a multi-leaf spring on the working conditions of a truck driver. *Eksploracja i Niezawodność – Maintenance and Reliability* 2021; 23 (3): 422–429, <http://doi.org/10.17531/ein.2021.3.3>.

## Evaluation of the influence of friction in a multi-leaf spring on the working conditions of a truck driver

Zdzisław Hryciów<sup>a</sup>, Wiesław Krasoń<sup>a\*</sup>, Józef Wysocki<sup>a</sup>

<sup>a</sup>Military University of Technology, Faculty of Mechanical Engineering, ul. Gen. Sylwestra Kaliskiego 2, 00-908 Warsaw, Poland

Indexed by:



### Highlights

- Suspension with a 3D model of spring, leaf interaction mechanism and variable friction forces.
- Evaluation of vibroisolation and energy dissipation in suspension models under changing driving conditions.
- Estimation of the level of nuisance and limitation of the permissible working time of the driver.
- The results can be applied to the diagnosis, design and testing of vehicle structures.

### Abstract

This article presents a simulation study of the suspension system in a vehicle that weighs approximately 12 tons (class N2). The authors have tested the influence of experimentally determined values of friction coefficients on the energy dissipated in the multi-leaf spring. The study was carried out using finite element analysis with LS-DYNA software. A nonlinear vibration model of the complete spring was developed, including the variable friction forces between the leaves. The model takes into account the sprung and unsprung mass of the chassis. Numerical tests were carried out using three different coefficients of friction (determined experimentally) for a selected speed of the car. Random realizations of the road micro-profile (type A, B, C) recommended by ISO 8608 were used. The results of the tests were presented in the form of acceleration curves in the vertical direction, comparative plots of daily vibration exposure A(8) and vibration transmission coefficient (T), and the distributions of RMS acceleration in frequency of one-third octave bands. This data was used to assess the quality of the vibration isolation system between the front suspension of the vehicle and the driver's seat.

### Keywords

seat vibration, vibroisolation, experimental-simulation research methodology, Finite Element Method (FEM), static and kinetic friction coefficient.

This is an open access article under the CC BY license (<https://creativecommons.org/licenses/by/4.0/>)

## 1. Introduction

In many areas of the world, dynamic and uncontrolled economic development causes irreversible degradation of the environment (climate change, pollution, degradation of natural water and land areas, including forest stands, etc.) [7]. Also, it can lead to the occurrence of pollution, in the form of smog, noise, vibration, etc. [5, 22]. Among the factors contributing to the creation of this pollution, road transport is shown to be the worst offender, despite the fact that it is also seen as an indicator of the economic development of the country [4]. The complex role of transport is an area of interest for many scientific and engineering communities, including civil engineering and transport, mechanical engineering and medical research teams [11].

A large number of vehicles are produced worldwide, and this is increasing every year [4]. The vehicles can be categorised in the N category (motor vehicles with at least four wheels, designed and constructed for the carriage of goods), including N1 – vehicles designed and constructed for the carriage of goods and having a maximum total mass not exceeding 3.5 t; N2 – vehicles designed and constructed for the carriage of goods and having a maximum total mass exceeding 3.5 t but not exceeding 12 t and N3 – vehicles designed and constructed

for the carriage of goods and having the maximum total mass exceeding 12 t.

The number of professional drivers is also increasing, who, in order to perform their professional activities, must not only be assessed as competent to drive the specific type of transport vehicle but also, due to the maintenance of the highest standard of road traffic safety (which is the direction of development of modern transport in many countries), be subjected to appropriate working conditions [20].

In their daily work, vehicle drivers are subjected to various effects of the environment in which they perform their activities. These include mechanical, physical, biological and chemical factors, which separately, and in combination, influence the functioning and reactions of the driver. The most adverse of them are vibration and noise – mechanical and physical hazards, respectively [12]. These hazards cause discomfort and sometimes – when excessively exposed – lead to the development of disease [13]. One area of the vehicle that combines both of these impacts is the suspension. Mechanical and acoustic waves are generated from the suspension. Friction plays a major role in their use, especially in the case of leaf springs. From an engineering point of view, due to friction, contact between components affects the

(\* ) Corresponding author.

E-mail addresses: Z. Hryciów - [zdzislaw.hryciow@wat.edu.pl](mailto:zdzislaw.hryciow@wat.edu.pl), W. Krasoń - [wieslaw.krason@wat.edu.pl](mailto:wieslaw.krason@wat.edu.pl), J. Wysocki - [jozef.wysocki@wat.edu.pl](mailto:jozef.wysocki@wat.edu.pl)

dynamic stiffness of the suspension and vehicle vibrations [24]. As a result of suspension deflection in the vertical direction, relative leaf movements in the spring and friction forces are created, which results in an increase in inelastic resistance in the suspension, this can worsen the driver's working conditions. Numerous scientific studies have shown that whole-body vibration (VBV – vibration dose values) of people operating various transport vehicles (drivers, operators, etc.) is associated with the onset and development of pain localized to the lumbosacral region of the spine (LBP).

The literature presents various models of elastic elements [2] (one-dimensional, two-dimensional or spatial), such as simple discrete models [3] and more complex numerical models [1] developed with the use of the finite element method (FEM) [8, 14] or special modeling techniques that are used to describe the vehicle suspension vibrations [19].

It is common practice, during the design or modernization of a motor vehicle, to simulate and test comfort parameters using models of varying degrees of complexity with varying computational accuracy.

Dukalski et al. examined the dynamics of the rear suspension system of a passenger car (mass  $\sim 1t$ ) with electric motors that are mounted in the rear wheel hubs [6]. A computational model was developed in the MSC.Adams environment. The basic parameters necessary to model the suspension, such as masses and corresponding mass moments of inertia, elastic-damping characteristics and tyre contact parameters, were determined experimentally. Road tests were used to validate the computational model. The study of the vertical dynamics of the suspension was limited to time and frequency analysis of the vibrations in the vertical direction. Root mean square (RMS) acceleration values and vibration exposure over time (VDV) were used to assess passenger comfort whilst driving. The results of preliminary simulation studies of the dynamics of a passenger car rear suspension system was presented, which confirm that a small change in the damping ratio significantly affected the dynamic characteristics of the suspension and resulted in a significant increase in the VDV index.

Numerical models for the evaluation of vehicle suspension quality and driver working conditions occupy a special place in the field of road transport. The paper [23] analyses the dynamic properties of a forest crane operator's seat for selected work cycles. A mathematical model was developed that considers the susceptibility of the operator's seat support, actuators and supports. The equations of motion of the crane model are based on the formalism of Lagrange's equations of motion of the second kind [23]. Two values of friction coefficients (Set-1 and Set-2) in mechanical joints were considered in the model. The values of force and friction coefficients were calculated using the LuGre friction model. The level of discomfort to the operator caused by the crane's vibration was estimated in accordance with the applicable standards for noise analysis and the impact of vibrations on the operator (N.V.H – Noise, Vibration and Harshness analyses). The simulation results obtained confirmed the large effect of friction on operator discomfort. The authors emphasized that the presented model can be modified to create advanced versions and other crane operating scenarios, which are necessary for detailed vibration and comfort analysis.

Researchers have carried out experimental studies examining the vibrations which affected twelve driver-operators, operating different types of special vehicles, equipped with lifting devices (front, rear, side and tilt frame) for municipal waste disposal [22]. Acceleration values were measured and recorded, using a Cartesian three-dimensional (3D) coordinate system, for the driver's seat and for the vertical direction on the cab floor. Changes in speed values and trajectories of vehicle movement during a typical work shift were also determined. The measurement results were analysed according to ISO 2631-1 [11]. In all cases, it was found that the daily vibration limit was exceeded, and it was indicated that impulsive vibrations were dominant in the analysed cycles. Significant intervention recommendations were proposed to mitigate their impacts. Ryan et al. investigated interventional transport of high-risk new-borns on a typical route between primary

and secondary care hospitals [21]. Experimental studies on the effects of mechanical vibrations and shocks to the whole body of a newborn infant during a typical road transport were performed. The studies were performed on three different types of roads (urban, main and highway) on a length of 32 km, with average vehicle speeds (20 km/h; 60 km/h and 100 km/h) for 46 min. A newborn infant (dummy) weighing 1.3 kg was transported in an ambulance using a traditional stretcher system with a mattress and a fluidized pad placed inside an infant protection cover (isolette). The results of the study showed that, regardless of the type of road, the daily permissible vibration limits were exceeded for all measurements. The frequency analysis showed that for all road types, low resonance of the car vibrations were 1 to 3 Hz and, for the dominant frequencies related to the road surface category, 7 Hz (urban), 12 Hz (main) and from 5 to 18 Hz (motorway). The results of the study clearly demonstrate that currently used ambulance equipment for transporting new-borns does not successfully mitigate the risk presented by road travel in the USA. The authors suggest that the future design of stretcher systems should eliminate vibrations in the range of 1 Hz to 3 Hz and extensively dampen vibrations from road irregularities and vehicle suspension in the range of 5 to 18 Hz.

Amrute et al. [1] and Hareesh et al. [8] have not considered the effect of variable friction between spring leaves which is caused by deflections of the suspension or the effect of static and kinetic friction coefficients on the amount of energy dissipated in the multi-leaf spring. Additionally, there is no information on the importance of vibroisolation between the front suspension of the vehicle and the truck driver's seat.

In this study, nonlinear analysis of a two-dimensional (2D) vibration model of a car with a dependent suspension is presented. The car weighs approximately 12 tons, and is equipped with a seven leaf (prototype) spring with mapped leaf geometry, together with the interaction mechanism of the leaf surfaces. Analysing the working conditions of the multi-leaf spring, it can be clearly observed that they change continuously during its operation [16]. Initially, there is usually a layer of graphite grease between the leaf springs, which is gradually removed during its lifecycle, as the leaf's work together. The process of removing the lubricant layer causes a change in the conditions of the leaf's interaction and, as a result, leads to the creation of dry friction conditions. Additionally, a layer of oxides appears on the surfaces of these components, the presence of which significantly worsens the conditions of interaction [9]. The model takes into account the state of the leaf's interacting surfaces, their velocities resulting from mutual displacement and variable values of friction forces caused by deflections of the suspension. The influence of static and kinetic friction coefficients on the amount of energy dissipated in the spring was estimated. Also, the influence of the coefficients on the quality of the vibroisolation system during the car movement on rough ground was analysed. Random road micro-profile characteristics (type A, B, C) were used to exert forces on the vehicle, for a constant car speed ( $v = 20$  m/s). Multivariate numerical studies were carried out using LS-DYNA [17]. In the simulation tests, the authors focused on the dynamic effects of the car's suspension which were caused by driving on selected roads, as well as the loads created in the car systems (components) – with particular attention to the driver's seat. The magnitude of vibrations transmitted from the road through to the suspension, to the car's support system, to the driver's seat is the basis of assessment of working conditions. Using the above information, two objectives of the research work were formulated. The first one was related to the experiment, determining the values of static and kinetic friction coefficients between spring leaves, and selected intermediate layers between interacting leaves. The second objective was the evaluation of the quality of the vibroisolation system between the front suspension of the vehicle and the driver's seat. The evaluation is based on the results of simulation tests, including the changes in the vertical component of acceleration, comparison of daily vibration exposure diagrams A(8) and changes of the vibration transmissibility coefficient (T), as well

as distributions of the effective values of acceleration in the vertical direction in the one-third octave bands.

## 2. Experimental determination of the friction coefficient

Tests were carried out using a laboratory test stand to measure the friction force for two types of friction pairs. A detailed description of the test stand has been described previously [9]. The advantage of the stand is that it makes it possible to observe the low velocities of relative motion of one element of the friction pair, fixed on a sliding table, in relation to the other one, held in a holder. The handle is connected via a load cell, to the frame of the test stand. A constant speed is maintained throughout the test. The change of normal load is achieved by changing the number of weights with known masses that are weighing down the tested elements.

Fragments of a leaf from a multi-leaf spring, designed for the front suspension of a car weighing about 12 tons, were used in the research. The fragments were made of 50HSA steel. The selected mechanical parameters of the material (sample) were as follows:  $R_m = 1086$  MPa (tensile strength);  $A_5 = 18.1\%$  (elongation);  $Z = 27.4\%$  (contraction);  $HB = 320$  (Brinell hardness);  $E = 2.03 \cdot 10^5$  MPa (Young's modulus).

The first friction pair was covered with a layer of rust, while the second was cleaned before the test. For each pair, the state of the intermediate layer, as well as the sliding velocity was changed. The tests were carried out with a vertical force of  $F = 107$  N. The relative sliding velocity was  $v_w = 0.0515$  mm/s;  $0.111$  mm/s;  $0.225$  mm/s and  $0.348$  mm/s respectively. In the first stage, the tests were conducted using dry surfaces. Next, the surfaces of the cleaned samples were covered with a layer of graphite grease. The surface conditions adopted for the tests correspond to the actual operating conditions of multi-leaf springs. Fig. 1 shows 3D images taken with a digital microscope (KEYENCE VHX-1000) of the surface of the samples covered with rust and partially cleaned.

Table 1. Selected surface roughness parameters for friction pair

Parameter [ $\mu\text{m}$ ]	Sample	
	Corroded	Cleaned
$R_{\text{max}}$	65.88	21.96
$R_z$	50.80	14.90
$R_a$	8.74	1.89
$R_t$	66.58	22.12
$W_a$	10.50	1.64

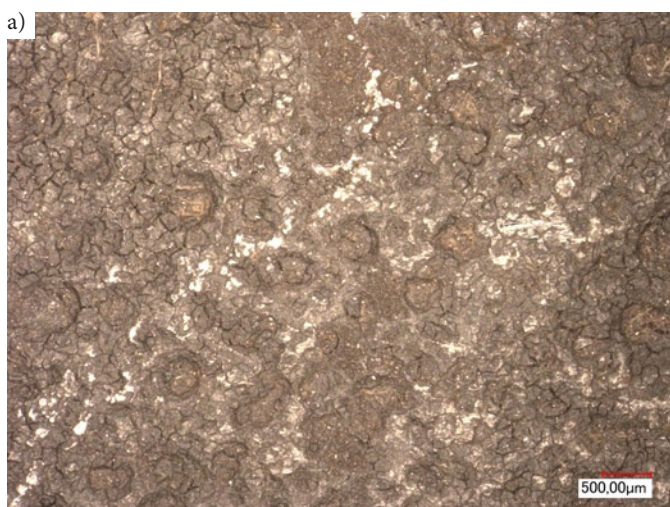


Fig. 1. View of sample surface (magnification  $\times 50$ ): a) covered with rust – maximum depth of surface roughness is  $65.88 \mu\text{m}$ , b) partially cleaned – maximum depth of surface roughness is  $21.96 \mu\text{m}$

The surface condition of friction pairs was evaluated on a laboratory test stand equipped with a HOMMELL TESTER T1000 contact profilometer for roughness determination. The measurements were conducted in two directions (longitudinal and perpendicular) on a section  $14.7$  mm long (elementary section equal to  $2.5$  mm), along which the measuring head moved at the speed of  $0.5$  mm/s.

Table 1 shows the basic roughness parameters for the friction pairs in corroded and cleaned condition. The results presented in the table are the arithmetic mean of five measurements. Analysing the results presented in Table 1, it should be noted that the maximum roughness heights ( $R_{\text{max}}$ ), the greatest heights of the profile ordinates ( $R_z$ ) and the total profile height ( $R_t$ ) for the cleaned sample are approximately one-third (ca. 33%) of the values determined for the corroded sample. In the case of other parameters, the differences are even greater. For a corroded sample, the  $R_a$  parameter is 4.6 times greater than for the cleaned sample, while the  $W_a$  index is as much as 6.4 times greater.

During the tests, the values of frictional force between the sample and the counter-sample were recorded for each variant. 3 to 5 repetitions were conducted. Fig. 2 shows examples of the friction force values for two friction pairs – for a sample with a corroded surface layer in a dry state and for a cleaned sample covered with graphite lubricant.

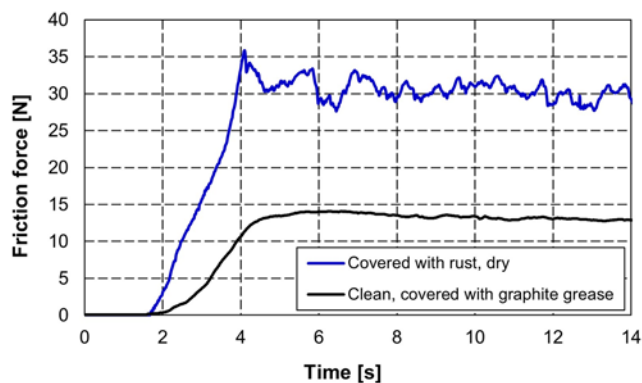


Fig. 2. Changes of the friction force value in time function for a corroded sample under dry friction conditions and a cleaned sample covered with graphite grease

The static ( $\mu_{s-sr}$ ) and kinetic ( $\mu_{k-sr}$ ) coefficients of friction were determined for each test on the basis of the recorded runs after relating the friction force to the applied normal load. Then, for several repetitions from each test variant, the arithmetic mean of the obtained results was calculated. The obtained average values of friction coefficients ( $\mu_{s-sr}$  and  $\mu_{k-sr}$ ) determined for the measurement series and the corre-

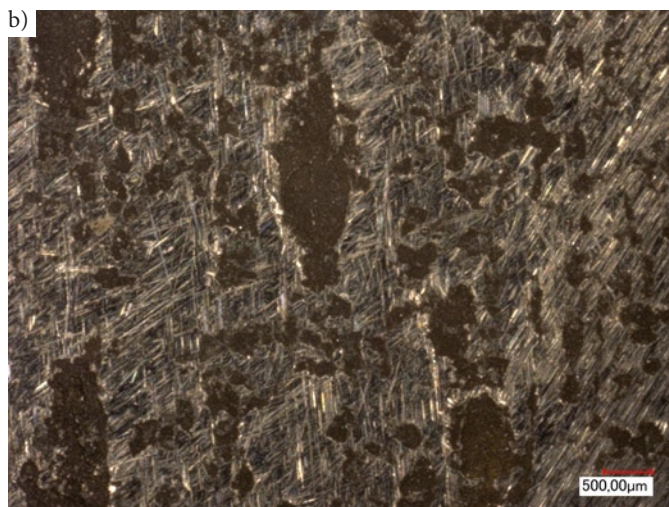


Table 2. Values of friction coefficients under a vertical force of  $F = 107\text{ N}$

Surface condition	Static coefficient of friction		Kinetic coefficient of friction	
	$\mu_{s-sr}$	$\sigma_{\mu s}$	$\mu_{k-sr}$	$\sigma_{\mu k}$
Dry, clean	0.151	0.0104	0.150	0.0080
Clean, coated with graphite grease	0.119	0.0092	0.120	0.0092
Rusty, dry	0.360	0.0438	0.310	0.0300

spending values of standard deviations ( $\sigma_{\mu s}$  and  $\sigma_{\mu k}$ ) are presented in Table 2. Analysing the results for cleaned surfaces, it should be stated that no significant effect of sliding velocity on the obtained values of static and kinetic friction coefficient is observed [9]. The reason is due to small changes in the relative velocity of the samples. The test stand allowed for measurement of velocities in the range of about 0.05 to 0.35 mm/s only. However, these values are close to the sliding velocity of the spring leaves in typical vehicle operation conditions.

### 3. Suspension simulation model

To simplify the simulation study, the distribution coefficient of the sprung masses ( $\epsilon$ ) according to (1) was assumed to be close to or equal to unity:

$$\epsilon = \rho^2 / (a_f \cdot b_r), \quad (1)$$

where:  $\rho$  – radius of inertia of the sprung masses of the car,  
 $a_f(b_r)$  – a distance of the sprung mass centre from the front (rear) axle.

Fulfilment of the above condition makes it possible to carry out independent analyses for front and rear suspension. Fig. 3 shows a nonlinear, plane vibration model of the frontal dependent suspension of a car. The car weighs approximately 12 tons and is equipped with a seven-leaf prototype spring with mapped leaf geometry, together with the interaction mechanism of the surfaces of the leaf's (variable friction forces). The seven-leaf spring was related to the sprung masses: the body and of the total mass of the seat with the driver, and to the unsprung mass of the chassis (tyre wheel, axle mass, and part of the spring mass). The vibration sub-systems: driver's seat and pneumatic tyres have discrete – linear elastic-damping characteristics. Eight-node solid elements were used to discretize the suspension. A contact was defined between the leaf's considering the friction forces. In the LS-DYNA system [17], the coefficient of friction is calculated based on the relation (2):

Table 3. Selected vibration parameters of the front truck suspension used in the model

No.	Parameter	Unit	Value
1	Body mass	kg	1,500
2	Axle mass with wheels	kg	310
3	Spring mass	kg	58.3
4	Seat and driver mass	kg	100
5	Tyre radial stiffness coefficient ( $k_t$ )	$\text{N}\cdot\text{m}^{-1}$	764,000
6	Tyre coefficient of damping ( $c_t$ )	$\text{N}\cdot\text{s}\cdot\text{m}^{-1}$	1,960
7	Suspension damping coefficient ( $c$ )	$\text{N}\cdot\text{s}\cdot\text{m}^{-1}$	7,500
8	Seat suspension stiffness coefficient ( $k_s$ )	$\text{N}\cdot\text{m}^{-1}$	10,000
9	Seat suspension damping coefficient ( $c_s$ )	$\text{N}\cdot\text{s}\cdot\text{m}^{-1}$	800

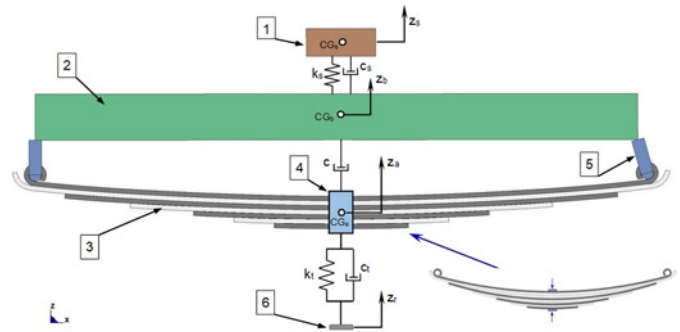


Fig. 3. Flat model of a car's dependent suspension: 1 – mass (seats mass + drivers' mass), 2 – mass of the body, 3 – seven leaf metal spring, 4 – unsprung mass, 5 –shackle, 6 – kinematic forcing of the road roughness profile ( $Z_r$ ), coordinates of vertical vibrations of the masses:  $Z_a$  ( $Z_b$ ,  $Z_s$ ) – unsprung (sprung, seat with driver),  $CG_b$  ( $CG_s$ ,  $CG_d$ ) – centre of the sprung mass (seat with driver, mass of the body)

$$\mu = \mu_k + (\mu_s - \mu_k) \cdot e^{-\gamma \cdot v_{rel}} \quad (2)$$

where:  $\mu_s$  – static coefficient of friction,  
 $\mu_k$  – kinetic coefficient of friction,  
 $\gamma$  – the exponent that determines the change of coefficients as a function of relative velocity,  
 $v_{rel}$  – relative velocity of interacting surfaces.

#### 3.1. Vibration parameters of the simulation model

The main parameters of the suspension model are shown in Table 3 – they were determined experimentally on the laboratory stands of the Institute of Vehicles and Transport – Faculty of Mechanical Engineering of the Military University of Technology.

#### 3.2. Scope of numerical model tests

The calculations were carried out in two stages. Due to the different radii of the individual leaves in the initial phase, it was necessary to grind them in the centre. This ensured that a pre-stress was induced and a simulation of interactive forces between the leaves was accounted for (generating, among other things, frictional forces, in the case of their mutual displacement in the horizontal direction). In the second stage, the accelerations of the spring, the body and the driver were determined whilst driving on uneven ground on a road that was characterise as average, good and very good condition. Under real conditions, the force is transmitted through the tyre wheel (with elastic and damping characteristics) to the drive axle. This was mapped by applying a kinematic excitation to the lower end of the spring ( $k_t$ ). It was generated according to the classification of road profiles presented in ISO 8608 [10], based on the power spectral densities of vertical displacements. This method of generating runs is commonly used in laboratory and simulation studies. The height of the unevenness of the road profiles

h can be treated as a realization of a random function, which is fully described by the power spectral density  $G_d(\Omega)$  [ $m^3/rad$ ]. Where  $\Omega$  [ $rad/m$ ] is the circular frequency described by the relation  $\Omega = 2\pi/L$ , where  $L$  is the roughness length. The equation for the power spectral density of roughness can be presented as follows:

$$G_d(\Omega) = G_d(\Omega_0)(\Omega / \Omega_0)^{-w} \quad (3)$$

where:  $G_d(\Omega_0)$  [ $m^3/rad$ ] – road roughness index,  
 $w$  – waviness index,  
 $\Omega_0$  – reference circular frequency.

According to ISO 8608 [10], when generating road irregularities, the circular frequency should be changed in the range of values from 0.069 rad/m to 17.77 rad/m. Table 4 shows the parameters of the analysed roads adopted for the calculations.

Table 4. Road parameters assumed for calculations [10]

Road class	$G_d(\Omega_0)$ ( $10^{-6} m^3/rad$ ), $\Omega_0 = 1 rad/m$ , $w = 2$		Road Quality Assessment
	Scope of Change	Geometric Mean	
A	<2	1	very good
B	2–8	4	good
C	8–32	16	average

Using the Matlab software, a programme was developed (according to ISO [10] and based on the parameters in Table 4) to generate the roughness profile for an assumed vehicle speed, length of the measurement section and road class. Figure 4 shows an example of the implementation of three road classes.

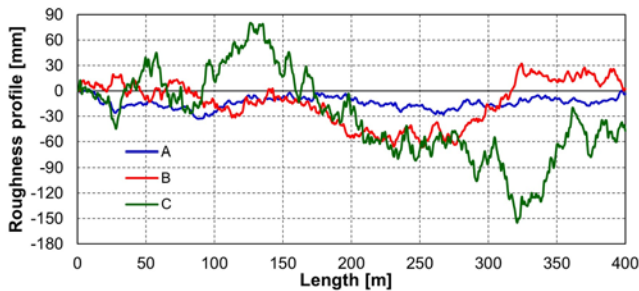


Fig. 4. Example of implementation of the roughness profile for a class A, B and C road

The quality of the suspension work (degree of vibroisolation) for different associations between the working spring leaf's (different values of friction coefficient) was determined by the vibration transmissibility coefficient (T) comparing the effective values of vibration accelerations:

$$T = \frac{RMS_b}{RMS_a} \quad (4)$$

where:  $RMS_a$  and  $RMS_b$  – RMS values of accelerations at points “a” (unsprung mass) and “b” (sprung mass).

Comparing the quality of suspension, one can also use a logarithmic scale to determine the vibroisolation efficiency (E) based on the relationship:

$$E = 20 \cdot \log\left(\frac{1}{T}\right) \text{ [dB]} \quad (5)$$

The evaluation of the level of vertical vibrations acting on the driver's seat was assessed, according to PN-EN 14253+A1 [20], on the

basis of daily vibration exposure value  $A(8)$ . Considering only vibrations in the vertical direction – it takes the form:

$$A(8) = k_z \sqrt{\frac{1}{T_0} \sum_{i=1}^n a_{ws}^2 \cdot t_i} \quad (6)$$

where:  $n$  – number of activities performed under vibration exposure,  
 $k_z = 1$  – weighting factor for Z direction,  
 $t_i$  – time of performing the i-th action,  
 $T_0$  – time of daily exposure (8 h),  
 $a_{ws}$  – frequency weighted acceleration of the driver's seat.

The following limits were used in the assessment: the exposure action value (EAV) – 0.5  $m/s^2$  and the daily exposure limit value (ELV) – 0.8  $m/s^2$ . Calculations were carried out for three variants of friction coefficients, corresponding to possible friction associations (states of spring leaf surfaces – clean and dry, covered with graphite grease, and covered with a thin layer of oxides). The values of static and kinetic friction coefficient (Table 2) adopted for the analysis were based on prior experimental research.

#### 4. Results

As a result of the numerical calculations, the values of the stress reduced according to the H-M-H energy hypothesis in individual leaf, deflection/displacement, velocities and accelerations of the spring and other components of the modelled suspension, the values of forces of interaction between individual leaf's were determined, as well as the values of the individual energies in the system (including the energy associated with the friction force). Figure 5 shows the distribution of the reduced stress H-M-H in the leaf springs when the vehicle moves at a speed of 20 m/s on a class C road (for selected time). The highest stress values occurred in the central part of the lower leaf spring. They are mainly caused by the leaf's being compressed by the yoke. The stress values are related to the mechanical properties of the structural material from which the spring is made, which can indicate the possibility of accelerated wear and even chipping of spring leaf tips due to fatigue effects. The distributions and changes of stress in leaf springs determined in this study can be used for fatigue analysis, in which it is possible to take into account the applied load spectrum, material characteristics of leaf springs and numerical estimation of main suspension component life on this basis, in the form of the acceptable number of load cycles until the occurrence of spring damage [3, 17, 18].

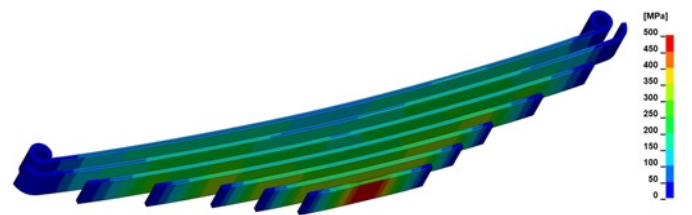


Fig. 5. Map of the H-M-H reduced stress in spring leaf's when the vehicle passes over a class C road with speed  $v = 20 m/s$

Fig. 6 shows the distribution of unit pressures caused by contact forces between spring leaves. From it, it can be concluded that the main interaction between the leaf's occurred at their ends. This is also confirmed by experimental observations in [15]. In these areas of the leaves, there is increased heating, as well as significant wear on their surfaces.

The vibroisolation properties of the different suspension stages are illustrated in Figure 7. It shows the vertical acceleration curves for the unsprung mass, sprung mass and the mass of the seat with the driver. They indicate a radical reduction of the acceleration ampli-

tude value, as well as a reduction of the vibrations of high-frequency components.

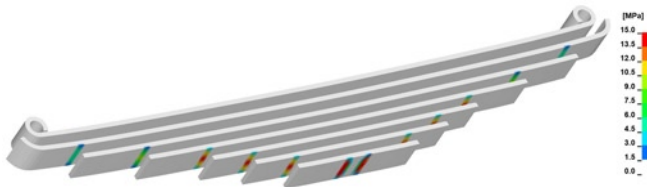


Fig. 6. Unit pressures between leaf springs when driving on a class C road with speed  $v = 20$  m/s

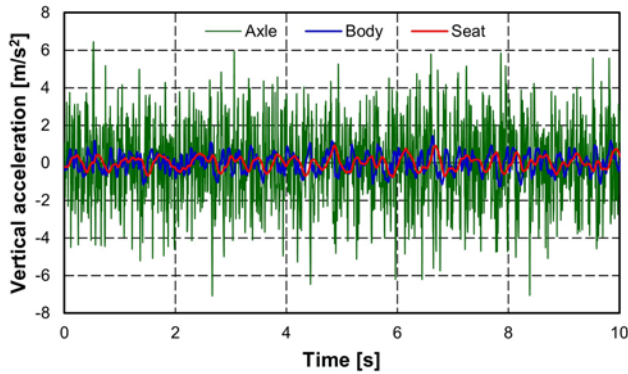


Fig. 7. Vertical acceleration during driving on road class A for coordinates (see fig. 3):  $Z_a$  (unsprung mass - axle),  $Z_b$  (sprung mass - body),  $Z_s$  (mass of the seat + driver - seat)

The magnitude of vibrations transmitted to the driver's seat depends on the conditions of interaction between the spring leaves (fig. 8). Reducing friction reduces the amount of vibration transmitted to the body. This phenomenon is particularly observable for roads with good pavement conditions. Increased resistances to the relative movement of the spring leaves can cause them to block temporarily. This results in increasing the acceleration value and the vibrations of higher frequency components.

Fig. 9 shows the calculated values of daily vibration exposure  $A(8)$  and vibration transmissibility coefficient (T). It is clear that the greatest differences between the calculated indices (for different values of friction coefficients) occur for the road with the best pavement condition. Deterioration of the road quality reduces the variation between the obtained results (Figure 9, Table 5).

The calculated value of daily exposure,  $A(8)$ , for springs with rust-covered surfaces increases in relation to those covered with graphite grease by as much as 38% (for a class B road, it is 13% and for a class C road, it is 3%). On the other hand, the vibration transmissibility coefficient (T) decreases respectively by 26% for class A roads, by 17% for class B and by 10% for class C. Table 5 presents the results obtained for the considered variants.

In addition to the results presented above, an analysis of the distribution of RMS values of accelerations in frequency one-third octave bands [11] was performed according to ISO standard [10]. It gives information about the strength of the vibration signal in the following

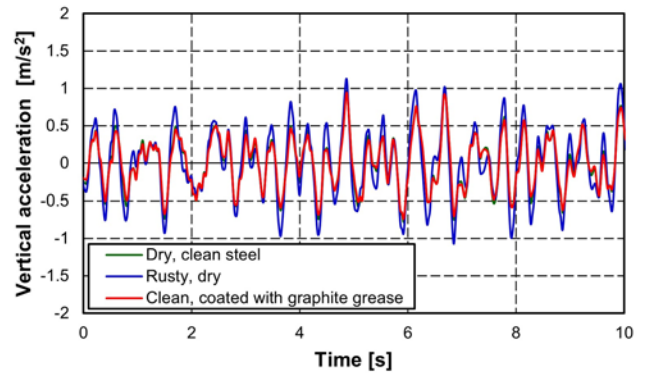


Fig. 8. Values of vertical acceleration for the  $Z_s$  coordinate (seat and driver mass) for three different associations (coefficients of friction) between the leaves when driving on a class A road with speed  $v = 20$  m/s

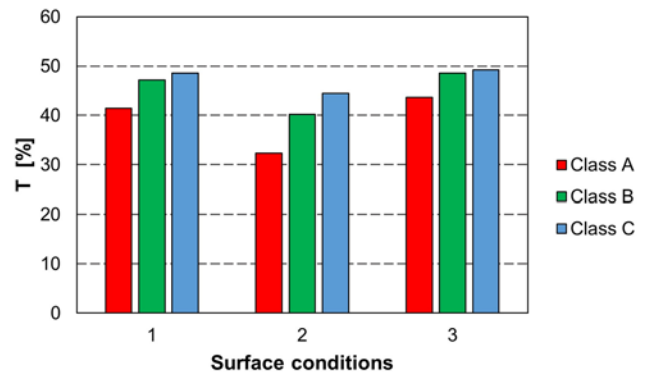
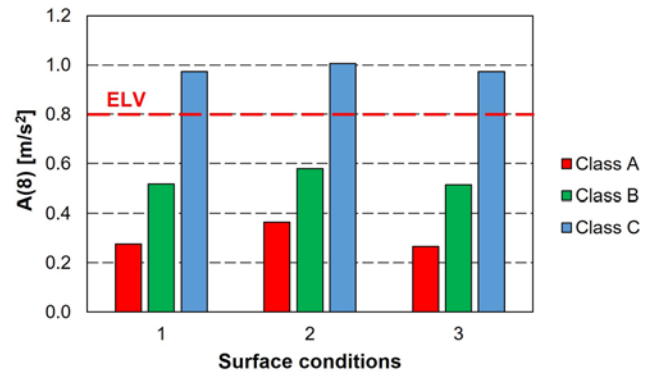


Fig. 9. Results of simulation tests: a) changes in daily vibration exposure  $A(8)$ , b) vibration transmissibility coefficient (T); 1 - cleaned friction pair tested in dry friction conditions, 2 - corroded friction pair tested in dry friction conditions, 3 - cleaned friction pairs covered with graphite grease, ELV - the daily exposure limit value

Table 5. Summary of results of simulation tests

Surface Condition	Road class								
	A			B			C		
	A(8) [m/s <sup>2</sup> ]	T [%]	E [dB]	A(8) [m/s <sup>2</sup> ]	T [%]	E [dB]	A(8) [m/s <sup>2</sup> ]	T [%]	E [dB]
dry, clean	0.276	41.5	-32.4	0.518	47.2	-33.5	0.973	48.6	-33.7
rust layer	0.365	32.3	-30.2	0.579	40.2	-32.1	1.006	44.4	-33.0
graphite grease	0.265	43.6	-32.8	0.514	48.5	-33.7	0.974	49.2	-33.8

frequency ranges. Figure 10 shows the obtained frequency distributions for roads of class A and C. In addition, the limits of exposure and the fatigue-decreased proficiency boundary levels are plotted. For

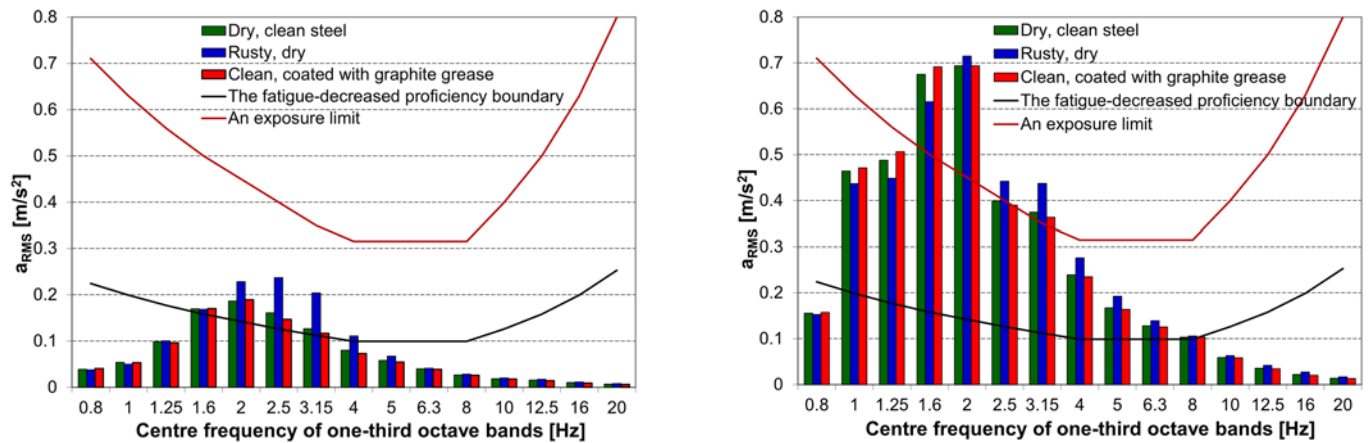


Fig. 10. Distribution of RMS values of vertical acceleration in one-third octave bands for three different associations (friction coefficients) between the leafs during driving with speed  $v = 20$  m/s, on roads: a) class A, b) class C

frequency ranges up to 1.6 Hz, the highest RMS values of the acceleration components are observed for the spring leafs that are coated with graphite grease. Above a frequency of 2 Hz, the highest values occur for the rust-covered leaf's surface. Increasing acceleration RMS values are particularly evident for the centre frequency bands of 2, 2.5 and 3.15 Hz when driving on a class A road. For a class C road, there was an exceedance of the exposure limit between 1.6 and 3.15 Hz. This means that the permitted working hours must be limited. This is consistent with the calculated A(8) index. Its values for all analysed frictional associations exceeded the daily exposure limit value (ELV)  $0.8 \text{ m/s}^2$  (Fig. 9).

## 5. Conclusions

The presented nonlinear, flat mathematical model of the dependent suspension of a car weighing about 12 tons, the proposal of its simplification, the method of discretization of the structure, the scope of research and the method of solution constitute a useful tool for creating new designs or modernizing existing dependent suspensions of motor vehicles.

Noteworthy is the developed program to generate a random road micro-profile according to ISO standards. The innovative element in the proposed model is the detailed reproduction of the spring geometry and the mechanism of interaction of the component leaf surfaces with the variable friction coefficients. The model considered the state of the mating surfaces of the leafs, their mutual displacement veloci-

ties and the variable magnitudes of friction forces that are caused by the deflections of the suspension during car movement on specific road classes. The research methodology and simulation model have some universal features, as they allow the evaluation of the driver's working conditions by determining the daily exposure to vertical vibrations A(8), the evaluation of the vehicle suspension quality in terms of vibration isolation (T) and its frequency structure. They also allow for the determination of the influence of dynamic actions on selected components of the suspension system, leading in effect to stress/strain distributions, which can be used in fatigue life prediction.

The applied research methodology and simulation models are novel and useful. They make it possible to evaluate the effectiveness of the vibration and energy dissipation system, with respect to different suspensions and driving conditions. For the conditions considered in the work, only for a class C road there was an exceedance of the exposure limit and the need to limit the driver's permitted hours of work.

The presented model can also be used for more detailed vibration and travel comfort analysis, e.g., in a bus or special vehicle. This can be developed by modifying the front suspension model into a vibration model of the whole vehicle, considering its geometric and vibrational parameters. Suspension testing methodology, simulation models and obtained results can be used both in diagnostics and for designing and testing new constructions of various types of vehicles.

## References

1. Amrute A V, Karlus E N, Rathore R K. Design and Assessment of Multi Leaf Spring. *International Journal of Research in Aeronautical and Mechanical Engineering Applications* 2013; 1(7): 115-124.
2. Atig A, Sghaier R B, Seddik R. A simple analytical bending stress model of parabolic leaf spring. *Proceedings of the Institution of Mechanical Engineers Part C: Journal of Mechanical Engineering Science* 2018; 232(10): 1838-1850, <https://doi.org/10.1177/0954406217709302>.
3. Borković P, Sustarsic B, Leskovek V, Zuzek B, Podgornik B, Malešević M. FEM simulation of a mono-leaf spring and its fatigue life prediction. *Structural Integrity and Life* 2012; 12(1): 53-57.
4. Directorate-General for Mobility and Transport (European Commission), Statistical pocketbook 2020. EU transport in figures. DOI10.2832/491038.
5. Du, BB., Bigelow, PL., Wells, RP., Davies, H., Hall, P., & Johnson, PW. The impact of different seats and whole-body vibration exposures on truck driver vigilance and discomfort. *Ergonomics* 2018; 61(4): 528-537, <https://doi.org/10.1080/00140139.2017.1372638>.
6. Dukalski P, Będkowski B, Parczewski K, Wnęk H, Urbaś A, Augustynek K. Dynamics of the vehicle rear suspension system with electric motors mounted in wheels. *Eksploatacja i Niezawodność - Maintenance and Reliability* 2019; 21 (1): 125-136, <https://doi.org/10.17531/ein.2019.1.14>.
7. European Council EUCO 10/20, CO EUR 8 CONCL 4, Brussels, 21 July 2020. 210720-euco-final-conclusions-en.pdf.
8. Hareesh K, Thillikkani S. Desing and Analysis of Leaf Spring - Using FEA Approach. *International Journal of Scientific Engineering and Technology (IJSET)* 2015; 4(3): 197-200, <https://doi.org/10.17950/ijset/v4s3/317>.
9. Hryciów Z, Krasoń W, Wysocki J. The experimental tests on the friction coefficient between the leaves of the multi-leaf spring considering a condition of the friction surfaces. *Eksploatacja i Niezawodność - Maintenance and Reliability* 2018; 20 (4): 682-688, <https://doi.org/10.17531/ein.2018.4.19>.

10. ISO 8608: 2016. Mechanical vibration - Road surface profiles - Reporting of measured data, <https://www.iso.org/standard/71202.html>.
11. ISO 2631-1: Mechanical vibration and shock - Evaluation of human exposure to whole-body vibration - Part 1: General requirements. International Organization for Standardization, 2018.
12. Jamroziak K, Kosobudzki M, Ptak J. Assessment of the comfort of passenger transport in special purpose vehicles. *Eksploracja i Niezawodność - Maintenance and Reliability* 2013; 15 (1): 25-30.
13. Kim J H, Aulck L, Hughes M, Zigman M, Cavallari J, Dennerlein J T, Johnson P W. Whole Body Vibration Exposures in Long-haul Truck Drivers. *Proceedings of the Human Factors and Ergonomics Society Annual Meeting 2016*; 59: 1274-1278, <http://doi.org/10.1177/1541931215591205>.
14. Kong Y S, Omar M Z, Chua L B, Abdullah S. Explicit Nonlinear Finite Element Geometric Analysis of Parabolic Leaf Springs under Various Loads. *Hindawi Publishing Corporation The Scientific World Journal* 2013; 2013(261926), 1-11, <https://doi.org/10.1155/2013/261926>.
15. Krason W, Wysocki J. Investigation of friction in dual leaf spring. *Journal of Friction and Wear* 2017; 38(3): 214-220, <https://doi.org/10.3103/S1068366617030096>.
16. Krason W, Wysocki J, Hryciow Z. Dynamics stand tests and numerical research of multi-leaf springs with regard to clearances and friction. *Advances in Mechanical Engineering* 2019; 11(5): 1-13, <https://doi.org/10.1177/1687814019853353>.
17. LS-DYNA, Keyword user's manual, Volume I, LS-DYNA R12, Livermore Software Technology (LST), AN Ansys Company, 07/17/20.
18. MSC.Software, What is Fatigue Analysis? MSC Nastran, <https://simulatemore.mscsoftware.com/what-is-fatigue-analysis-msc-nastran/25.03.2021>.
19. Padmakar S, Seyd A H. Design and Analysis of Leaf Spring for Tanker trailer suspension System. *Global Journal of Advanced Engineering Technologies* 2015; 4(3): 240-250.
20. PN-EN 14253+A1:2011, Mechanical vibrations - Measurement and calculation of occupational exposure to vibrations with a general effect on the human body for the purposes of health protection, Practical guidelines, 2011. (in Polish)
21. Ryan D M, Lokeh A, Hirschman D, Spector J, Parker R, Johnson P W. The effect of road type on neonate whole body vibration exposures during ambulance transport. *7th American Conference on Human Vibration* 2018; 76-77.
22. Ryou H, Johnson P W. Whole-Body Vibration Exposures Among Solid Waste Collecting Truck Operators. *Proceedings of the Human Factors and Ergonomics Society Annual Meeting 2018*; 62(1): 860-864, <https://doi.org/10.1177/1541931218621196>.
23. Urbaś A, Szczotka M. The influence of the friction phenomenon on a forest crane operator's level of discomfort. *Eksploracja i Niezawodność - Maintenance and Reliability* 2019; 21 (2): 197-210, <https://doi.org/10.17531/ein.2019.2.3>.
24. Zhou Z, Guo W, Shen T, Wang F, Ju J, Wang H, Song E. Research and Application on Dynamic Stiffness of Leaf Spring. *SAE - China, FISITA Proceedings of the FISITA 2012 World Automotive Congress. Lecture Notes in Electrical Engineering* 2012; 198: 105-119, [https://doi.org/10.1007/978-3-642-33795-6\\_10](https://doi.org/10.1007/978-3-642-33795-6_10).